Individual differences in functional brain connectivity predict temporal discounting preference in the transition to adolescence

Jeya Anandakumar*[1], Kathryn L. Mills*[2], Eric Earl[1], Lourdes Irwin[1], Oscar Miranda-Dominguez[1], Damion V. Demeter[5], Alexandra Walton-Weston[1], Sarah Karalunas[3], Joel Nigg[3], Damien A. Fair[1,3,4]

[1] Department of Behavioral Neuroscience, Oregon Health & Science University, Portland, OR
[2] Department of Psychology, University of Oregon, Eugene, OR
[3] Department of Psychiatry, Oregon Health & Science University, Portland, OR
[4] Advanced Imaging Research Center, Oregon Health & Science University, Portland, OR
[5] Department of Psychology, University of Texas at Austin, Austin, TX

*Contributed equally to this work

Corresponding Author:
Kathryn L. Mills
University of Oregon
115 Lewis Integrative Sciences
Eugene OR, 97403
Phone: 541 346 4905
Email: kathryn.l.mills@gmail.com

Abstract

The transition from childhood to adolescence is marked by distinct changes in behavior, including how one values waiting for a large reward compared to receiving an immediate, yet smaller, reward. While previous research has emphasized the relationship between this preference and age, it is also proposed that this behavior is related to circuitry between valuation and cognitive control systems. In this study, we examined how age and intrinsic functional connectivity strength within and between these neural systems relate to changes in discounting behavior across the transition into adolescence. We used mixed-effects modeling and linear regression to assess the contributions of age and connectivity strength in predicting discounting behavior. First, we identified relevant connections in a longitudinal sample of 64 individuals who completed MRI scans and behavioral assessments 2-3 times across ages 7-15 years (137 scans). We then repeated the analysis in a separate, cross-sectional, sample of 84 individuals (7-13 years). Both samples showed an age-related increase in preference for waiting for larger rewards. Connectivity strength within and between valuation and cognitive control systems accounted for further variance not explained by age. These results suggest that individual differences in functional neural organization can account for behavioral changes typically associated with age.

Keywords: delay discounting, fMRI, intrinsic connectivity, longitudinal, resting state

Introduction

Temporal discounting (also known as inter-temporal choice or delay discounting) is the process of assessing the value of waiting for a future reward depending on the magnitude of the reward and the delayed time. Individuals vary in their temporal discounting behavior, with some having a stronger preference for taking a smaller immediate reward versus waiting for a larger reward, and vice versa (Sadaghiani & Kleinschmidt, 2013). Previous experimental studies suggest a positive relationship between chronological maturation (age) and the tendency to prefer waiting for the larger reward (de Water, Cillessen, & Scheres, 2014; Steinberg et al., 2009), although some studies have found evidence for a nonlinear relationship in the transition into adolescence (Scheres, Tontsch, Thoeny, & Sumiya, 2014). Interestingly, the development of temporal discounting with age may be a stable marker of liability for disinhibitory psychopathologies such as ADHD even when psychopathological symptoms change with age (Karalunas et al., 2017). It has been proposed that brain function and organization can explain individual differences in temporal discounting behavior (Christakou, Brammer, & Rubia, 2011; Hare, Hakimi, & Rangel, 2014; Li et al., 2013; Scheres, de Water, & Mies, 2013; van den Bos, Rodriguez, Schweitzer, & McClure, 2014). Therefore, in this study, we analyzed how chronological maturation interacts with functional brain organization to predict temporal discounting.

Temporal discounting as a measure of decision-making preference

Tasks assessing temporal discounting behavior can be used to measure an individual's preference for a smaller-sooner reward (SSR) in comparison to a larger-later reward (LLR) (Green, Myerson, & Mcfadden, 1997). These tasks typically require individuals to choose between two rewards that vary in both the reward size and the delay time required until the amount is acquired

(Myerson & Green, 1995). For example, participants typically respond to several questions in the following format: "At the moment, what would you prefer?" Below the question two options are presented (e.g. "$7.00 now", "$10 in 30 days"). The SSR and LLR vary in both delay interval and reward size over successive trials; this way, the subjective value of temporal reward can be measured. Individuals preferring the SSR are characterized to have steeper temporal discounting; conversely, individuals preferring the LLR are characterized to have less temporal discounting. One way to measure this subjective value of temporal reward is through the use of indifference points (the delay duration at which the magnitude of SSR equals the magnitude of LLR) (Richards, Zhang, Mitchell, & de Wit, 1999). The indifference points are useful in calculating a single index of discounting rate, and in determining the value of the delayed reward (Yi, Pitcock, Landes, & Bickel, 2010). Specifically, plotting the indifference points in a series yields a discount curve, which describes the rate at which the value of reward decreases as time is increased.

Neural networks involved in temporal discounting

Previous studies have shown that cortico-striatal circuitry is greatly involved in decision-making processes (Haber & Knutson, 2009), including temporal discounting (Peters & Büchel, 2011). In the present study, we focus on two cortico-striatal systems (defined *a priori*) that have been consistently correlated with different outcomes of an individual's preference and value (Peters & Büchel, 2011; van den Bos et al., 2014): a valuation system (amygdala, medial orbitofrontal cortex, posterior cingulate cortex, ventromedial prefrontal cortex, and ventral striatum) and a cognitive control system (ventral lateral prefrontal cortex, dorsal anterior cingulate cortex, dorsolateral prefrontal cortex, dorsal striatum, and inferior frontal cortex) (See Figure **1a**). We

also assessed connectivity between these networks and the supplementary motor area and hippocampus, given their involvement in intertemporal choice behavior (Peters & Büchel, 2010; Scheres et al., 2013; van den Bos et al., 2014). Overall, it has been theorized that adults with high temporal discounting preference are more likely to show greater recruitment of the control network and less recruitment of the valuation network when choosing a LLR over a SSR (van den Bos & McClure, 2013; Volkow & Baler, 2015).

Neural networks involved in temporal discounting can be interrogated with MRI in multiple ways, including task-based fMRI studies in which participants are asked to make temporal discounting decisions, and as well as in studies that compare anatomical or functional connectivity to temporal discounting preferences measured outside of the scanner. Previous studies have examined structural connectivity (white matter fiber integrity) and its relation to temporal discounting through Diffusion Tensor Imaging (DTI). Increased structural connectivity between the striatum and cortical control regions have been found to be related to decreased temporal discounting, whereas increased structural connectivity between the striatum and subcortical valuation regions were related to increased temporal discounting in adults (van den Bos et al., 2014).

While task-evoked brain activity can inform us on the functionality of cortical networks during specific contexts, intrinsic brain activity at rest can be used to measure an individual's functional brain organization. The intrinsic activity of the brain reflects, in part, past activities, and these fluctuations impact future behavior (Sadaghiani & Kleinschmidt, 2013). Brain functionality and fluctuations are believed to determine and shape connectivity patterns. Here we study the brain's

intrinsic connectivity using resting-state functional connectivity MRI (rs-fcMRI) (Power, Schlaggar, & Petersen, 2014). rs-fcMRI measures the functional relationship between regions while the participant is not performing a specific task by measuring slow, spontaneous fluctuation of the blood oxygen level dependent (BOLD) signal. Intrinsic activity measures reveal the cohesive connections and interactions present in neuronal networks (Boly et al., 2008). Previous studies in adults have found that intrinsic brain connectivity within cortico-striatal networks were related to an individual's temporal discounting preference (Calluso, Tosoni, Pezzulo, Spadone, & Committeri, 2015; Li et al., 2013).

Development of neural networks underlying temporal discounting

It is hypothesized that differential rates of maturation across cortico-striatal systems, and the protracted development of the interconnections between them, are related to changes in behavior across development (Casey, 2015; Costa Dias et al., 2012, 2015; van den Bos, Rodriguez, Schweitzer, & McClure, 2015). In adults, it has been theorized that greater recruitment of control networks (and less recruitment of the valuation networks) are indicative of choosing the LLR, however, it is currently unclear if this brain-behavior relationship is present throughout development. One of the first task-based fMRI studies of temporal discounting examined the impact of age-related (ages 12-32 years; males) changes in brain activation when deciding between a SSR and a LLR (Christakou et al., 2011). This study demonstrated that when choosing an immediate reward, *increased* recruitment of the vmPFC and *decreased* recruitment of the ventral striatum, insula, anterior cingulate, occipital, and parietal cortices was related to increasing age and preference for LLR. Further, greater coupling between the ventral striatum and vmPFC was also related to increasing age and preference for LLR, suggesting that increased

functional connectivity between the vmPFC and ventral striatum (regions of the valuation network) might be one neural mechanism underlying developmental changes in the preference for delayed rewards.

Another theory is that neural systems involved in three cognitive processes: valuation (i.e., the value placed on a certain stimuli or outcome), cognitive control (i.e., engaging in goal-directed cognitive processes), and prospection (i.e., thinking about the future), are involved in the process of temporal discounting (Peters & Büchel, 2011). Using this framework, Banich et al. (2013) compared the behavioral and neural correlates of temporal discounting in younger (14-15 years) and older (17-19 years) adolescents, and how these measures related to an individual's self-reported tendency to think beyond the present. Behaviorally, older adolescents were more likely to choose a delayed reward over an immediate reward, and were slower than younger adolescents to choose the immediate reward (Banich et al., 2013). The pattern of brain activity related to intertemporal decision making was more distinct when choosing between immediate versus delayed rewards in the older adolescents compared to the younger adolescents (Banich et al., 2013). Across groups, individuals who reported a greater tendency to think beyond the present showed decreased recruitment of cognitive control regions during the temporal discounting task. These results suggest that both age and individual differences are related to the neural processing of temporal discounting.

Another study found that greater white matter integrity in pathways connecting the frontal and temporal cortices with other areas of the brain were positively correlated with the preference for delayed rewards across ages 9-23 years (Olson et al., 2009). Some of these correlations were

159 developmentally related, whereas some of the effects appeared to be age-independent. For
160 example, the relationship between greater white matter integrity in right frontal and left temporal
161 regions and increased preference for delayed reward was not attributable to age. However, the
162 relationship between integrity of white matter in left frontal, right temporal, right parietal (as
163 well as some subcortical-cortical circuits) and the preference for delayed reward was age-related,
164 as these white matter tracts also increased in integrity across the age range studied. These results
165 show that both age and individual differences in neural circuitry are related to an individual's
166 preference for immediate versus delayed rewards. Another study examined the relationship
167 between temporal discounting and fronto-striatal circuitry in a longitudinal study of individuals
168 between the ages of 8-26 (Achterberg, Peper, van Duijvenvoorde, Mandl, & Crone, 2016). This
169 study found that preference for LLR increased non-linearly between childhood and early
170 adulthood, and that greater fronto-striatal white matter integrity was related to the preference for
171 LLR (Achterberg et al., 2016).
172
173 Taken together, these studies demonstrate that people, on average, show increasing preference to
174 wait for larger rewards rather than take immediate (smaller) rewards as they get older, but the
175 increase may be nonlinear. Individual differences across development in temporal discounting
176 preference are related to differences in functional neural organization. How one comes to choose
177 a smaller immediate reward over a larger distant reward could be related to how that individual
178 values the proposed reward, or it could be related to how well that individual can inhibit
179 reflexive urges or the ability to think about the future. The development of brain systems
180 involved in evaluating rewards, cognitive control, and thinking about the future all appear to

contribute to the developmental changes in how we process situations that involve us making a choice between an immediate outcome and a distant outcome.

Current study

This current project examines how developmental changes in functional connectivity between and within the cognitive control network, valuation network, hippocampus and SMA relate to temporal discounting preferences during the transition into adolescence. Specifically, we tested to see if changes in functional connectivity strength could explain additional variance in temporal discounting preferences above chronological age. Previous studies have reported no significant difference in discounting behavior between boys and girls (Cross, Copping, & Campbell, 2011; Lee et al., 2013), suggesting any sex effects are likely to be small. Therefore, to conserve statistical power, the relationship between sex and temporal discounting behavior was not examined.

Methods

Participants

Our two neurotypical samples were drawn from an ongoing longitudinal project examining brain development in children, recruited from the community, with and without attention-deficit/hyperactivity disorder (ADHD). Our first sample consisted of 64 individuals with 2 or 3 longitudinal scans each (n=137 scans) and our second cross-sectional sample consisted of 84 individuals. Details for both samples are included in **Table 1**. All participants were typically-developing children without psychiatric diagnoses and exhibited typical neurological patterns of thoughts and behavior throughout the study. Psychiatric status was evaluated based on

evaluations with the Kiddie Schedule for Affective Disorders and Schizophrenia (KSADS; Puig-Antich & Ryan, 1986) administered to a parent; parent and teacher Conners' Rating Scale-3rd Edition (Conners, 2003); and a chart review a child psychiatrist and neuropsychologist that required agreement. Any participant who was identified as having a current psychiatric, neurological, or neurodevelomental disorder was excluded from the present study. IQ was estimated with a three-subtest short form (block design, vocabulary, and information) of the Wechsler Intelligence Scale for Children, 4th Edition (Wechsler, 2003).

Table 1. Participant demographic characteristics for each sample.

	Longitudinal Sample Characteristics			**Cross-sectional Sample Characteristics**		
	All	Female	Male	All	Female	Male
N	64	23	41	84	42	42
Age mean (SD)	10.8 (1.83)	10.6 (1.95)	10.9 (1.77)	10.3 (1.39)	10.3 (1.34)	10.3 (1.44)
Age range	7.3-15.7	7.3-15.7	7.5-14.5	7.3-13.3	8-13.3	7.2-13.2
AUC mean (SD)	0.51 (0.273)	0.51 (0.261)	0.51 (0.281)	0.45 (0.288)	0.44 (0.306)	0.47 (0.273)
AUC range	0.04 - 1	0.07 - 0.99	0.04 - 1	0.02 - 0.98	0.03 - 0.98	0.02 - 0.98
IQ mean (SD)	115.3 (13.95)	116.6 (9.58)	114.6 (15.88)	116.5 (13.82)	114.5 (14.86)	118.4 (12.59)
IQ range	72 - 144	98 - 132	72 - 144	78 - 148	78 - 144	96 - 148
N visits	137	49	88	84	42	42
2 visits	55	20	35	-	-	-
3 visits	9	3	6	-	-	-

Temporal Discounting task

The temporal discounting task evaluates personal preference for a hypothetical delayed or immediate reward. Participants were presented a computerized task with a series of questions, and were read the following instruction before proceeding to the task:

For the next task, you can choose between two options by clicking on it using the computer mouse. You can change your selection as often as you would like. Once you have decided which option you prefer, you can go on to the next question by clicking on the 'next question' box. One option will always be some amount of money available now. The other option will always be some amount of money later. The waiting period will vary between now and 180 days. Imagine that the choices you make are real– that if you choose 'money now' you would receive that amount of money at the end of the task and that if you choose 'money later' that you would actually have to wait before receiving the money. So, what are you going to do?

The computer-based task consisted of 92 questions with an option to get a reward immediately or get a larger amount of money ($10.00) at a later time period. Most of the participants were presented delays in intervals of 7, 30, 90, 180 days; a small percent of the participant were presented with different delay intervals of 1, 7, 30, 90 days.

Our temporal discounting task was analyzed by multivariate mathematical equations to measure an individual's decision-making preference. Reward in relation to the time span is usually used to measure the preference of an individual or a collective population generalized by age. There are many mathematical ways to analyze temporal discounting task, however, for this experiment we choose Area Under Curve (AUC). AUC (see **Box 1**) best represents the preference of the participants as it takes into consideration the indifference point and the corresponding delay time (Myerson, Green, & Warusawitharana, 2001). AUC is equated to best represent the variables present in this experiment; it takes into account the sum of indifference

241 and delay points acquired through temporal discounting, and outputs one value making it easier
242 for analysis (Myerson et al., 2001).
243
244 Box 1. AUC Equation

$$AUC = \sum (x_2 - x_1) \left[\frac{y_1 + y_2}{2} \right]$$

245
246
247 The x_2 and x_1 are the delayed points, and y_2 and y_1 represent the indifference points that
248 correspond to the delays (Hamilton et al., 2015; Odum, 2011). The AUC outputs a signal value
249 between 0 and 1; the lower the number represents the greater possibility to disregard the value of
250 the reward, and have less tolerance for the delay time (Myerson et al., 2001; Odum, 2011). The
251 AUC values and temporal discounting are inversely proportional, the closer the AUC value is to
252 zero the more temporal discounting is present, therefore the participant is least likely to wait for
253 a bigger reward. Likewise, the farther away the AUC value is to zero the most likely the
254 participant is going to wait for the larger reward to be received at a later time.
255
256 Three validity criteria were applied to the quantification of AUC. The first criterion was to make
257 sure that an indifference point for a specific delay was not greater than the preceding delay
258 indifference point by more than 20% or $2 (Johnson & Bickel, 2008). The next criterion was the
259 requirement for the final indifference point, at 180 days, to be less than the first indifference
260 point, at 0 days, to indicate variation in subjective value of rewards across (Johnson & Bickel,
261 2008). The final criterion was to require the first, at 0 day, indifference point to be at least 9.25.
262 This last criterion was enforced because a lower value indicates that the participant chose

multiple time to receive the smaller "now" over the larger "now", suggesting poor task engagement of misunderstanding of the task (Mitchell, Wilson, & Karalunas, 2015).

MRI acquisition

MRI was acquired using a 3.0 Tesla Siemens Magnetom Tim Trio scanner with a twelve-channel head-coil at the Oregon Health & Science University Advanced Imaging Research Center. One high-resolution T1-weighted MPRAGE (TR=2300ms, TE=4ms, FOV=240x256mm, 1mm isotropic, sagittal acquisition) and multiple T2-weighted echo planar imaging (TR=2500ms, TE=30ms, FOV = 240x240mm, 3.8mm isotropic, either 82 or 120 volumes, axial acquisition, 90° flip angle) series were acquired during each scan visit. Functional data were collected at rest, in an oblique plane (parallel to anterior commissure-posterior commissure plane), and steady state magnetization was assumed after five frames (~10s). Participants were instructed to stay still and fixate their gaze on a standard fixation-cross in the center of the display during the acquisition of resting state scans.

Image processing

The data were processed following the minimum processing steps outlined by the Human Connectome Project (Glasser et al., 2013), which included the use of FSL (Jenkinson, Beckmann, Behrens, Woolrich, & Smith, 2012; Smith et al., 2004; Woolrich et al., 2009) and FreeSurfer image analysis suite (http://surfer.nmr.mgh.harvard.edu/) (Dale, Fischl, & Sereno, 1999; Fischl, Sereno, & Dale, 1999). With this method, gradient distortion corrected T1w and T2w volumes are first aligned to MNI's AC-PC axis and then nonlinearly normalized to the MNI atlas. Next, the T1w and T2w volumes are re-registered using boundary based registration

(Greve & Fischl, 2009) to improve alignment. The brain of each individual is then segmented using the 'recon-all' FreeSurfer functions, which are further improved by utilizing the enhanced white matter-pial surface contrast of the T2w sequence. The initial pial surface is calculated by finding voxels that are beyond ± 4 standard deviations from the grey matter mean. The resulting parameter is then used to make sure no lightly myelinated grey matter is excluded. The estimated segmentation is refined further by eroding it with the T2w volume. Of the 221 total scan visits included in this study, 51 (23%) were processed without a T2w volume, either because this sequence was not acquired or was judged as being of low quality. These 51 were processed using FreeSurfer's regular T1 segmentation algorithm (Fischl et al., 2002). Next, the preliminary pial surface and white matter surface are used to define an initial cortical ribbon. The original T1w volume is smoothed with the ribbon using a Gaussian filter with a sigma of 5mm. Then, the original T1w image is divided by the smoothed volume to account for low frequency spatial noise. This filtered volume is used to recalculate the pial surface, but now using 2 (instead of 4) standard deviations as threshold to define the pial surface. These segmentations are then used to generate an individualized 3D surface rendering of each individual, which is finally registered to the Conte 69 surface atlas as defined by the Human Connectome Project. This registration process allows all data types (cortical thickness, grey matter myelin content, sulcal depth, function activity, functional and structural, connectivity, etc.) to be aligned directly within and between individuals. All T1w and T2w MRI scans were quality controlled for any noticeable movement through visual inspection of raw and reconstructed images. The images were assessed in a pass or fail manner; scans that failed were excluded from the samples included in the present study.

Functional EPI data are registered to the first volume using a 6-degrees of freedom linear registration and correcting for field distortions (using FSL's TOPUP), except for two scans (of 221) where no field map had been acquired. Next the EPI volumes are averaged, with each volume of the original time series re-registered to the average EPI volume using a 6-degrees of freedom linear registration. This last step avoids biases due to a single frame being used, which may be confounded by variability of movement across a given run. The average EPI volume is then registered to the T1w volume. The matrices from each registration step are then combined, such that each frame can be registered to the atlas all in a single transform (i.e. only one interpolation).

The resulting time-courses are then constrained by the grey matter segmentations and mapped into a standard space of 91,282 surface anchor points (greyordinates). This process accounts for potential partial voluming by limiting the influence of voxels that "straddle" grey and non-grey matter voxels (pial surface, white matter, ventricles, vessels, etc). Two thirds of the greyordinates are vertices (located in the cortical ribbon) while the remaining greyordinates are voxels within subcortical structures. Thus, the BOLD time courses in greyordinate space are the weighted average of the volume's time courses in grey matter, where the weights are determined by the average number of voxels wholly or partially within the grey matter ribbon. Voxels with a high coefficient of variation are excluded. Next, the surface time courses are downsampled to the greyordinate space after smoothing them with a 2mm full-width-half-max Gaussian filter.

The additional preprocessing steps necessary for resting-state functional connectivity analyses consist of regressing out the whole brain (in this case the average signal across all greyordinates

(e.g., see Burgess et al., 2016), ventricle and white matter average signal, and displacement on the 6 motion parameters, their derivatives and their squares (Power, Mitra, et al., 2014). All regressors are individualized and specific to the participant, based on their own segmentations. The regression's coefficients (beta weights) are calculated solely on the frames where the frame displacement is below 0.3mm to reduce the influence of movement "outliers" on the output data, but all the time courses are regressed to preserve temporal order for temporal filtering. Finally, time courses are filtered using a first order Butterworth band pass filter with cutting frequencies of 9 millihertz and 80 millihertz.

We applied a strict motion censoring procedure to the resting-state images (Fair, Nigg, et al., 2012; Power, Barnes, Snyder, Schlaggar, & Petersen, 2012) which takes the absolute value of the backward-difference for all rotation and translation measures in millimeters, assuming a brain radius of 50mm, and summates those absolute backward-differences for a measure of overall framewise displacement (FD). Volumes with a displacement exceeding 0.2mm were excluded, and we also removed frames with less than five contiguous frames of low motion data between instances of high motion (FD > 0.2mm) data to confidently account for motion effects on adjacent volumes (Power, Mitra, et al., 2014). Only participants with greater than 5 minutes of high quality data were included in the present analysis. The mean framewise displacement of participants in the first sample was 0.08 ± 0.02mm; range 0.05 - 0.13mm. The mean framewise displacement of participants in the second sample was 0.09 ± 0.02mm; range 0.04 - 0.13mm. More information on the motion characteristics on the full sample (i.e. including those excluded) can be viewed in Dosenbach et al., (2017).

355 *Regions of interest*

356 Our regions of interest (ROIs) included regions within valuation and cognitive control systems,
357 as well as hippocampus and supplementary motor area (SMA). For our cortical ROIs, we
358 selected regions within each of these networks from the Deskan-Killiany atlas provided by
359 FreeSurfer (Desikan et al., 2006). While other parcellations can be considered, we chose this
360 parcellation in order to examine anatomically-defined cortical regions that have been identified
361 in previous work. Cortical reconstruction and volumetric segmentation was performed with the
362 FreeSurfer image analysis suite, which is documented and freely available for download online
363 (http://surfer.nmr.mgh.harvard.edu/). The technical details of these procedures are described in
364 prior publications (Dale et al., 1999; Fischl et al., 2002; Fischl & Dale, 2000). FreeSurfer uses
365 individual cortical folding patterns to match cortical geometry across subjects (Fischl et al.,
366 1999), and maps this parcellation of the cerebral cortex into units with respect to gyral and sulcal
367 structure (Desikan et al., 2006; Fischl et al., 2004). Our striatal and subcortical ROIs were
368 defined based on FreeSurfer's anatomical segmentation procedure. For the purposes of this study
369 we examined the nucleus accumbens (NAcc), pallidum, amygdala, medial orbitofrontal cortex
370 (mOFC), and posterior cingulate cortex (PCC) as part of the valuation network, and the caudate,
371 putamen, anterior cingulate cortex (ACC), dorsal anterior cingulate cortex (dACC), dorsolateral
372 prefrontal cortex (dlPFC), inferior frontal gyrus (IFG), and ventrolateral prefrontal cortex
373 (vlPFC) of the cognitive control network (**Figure 1; SI Table 1**).

374

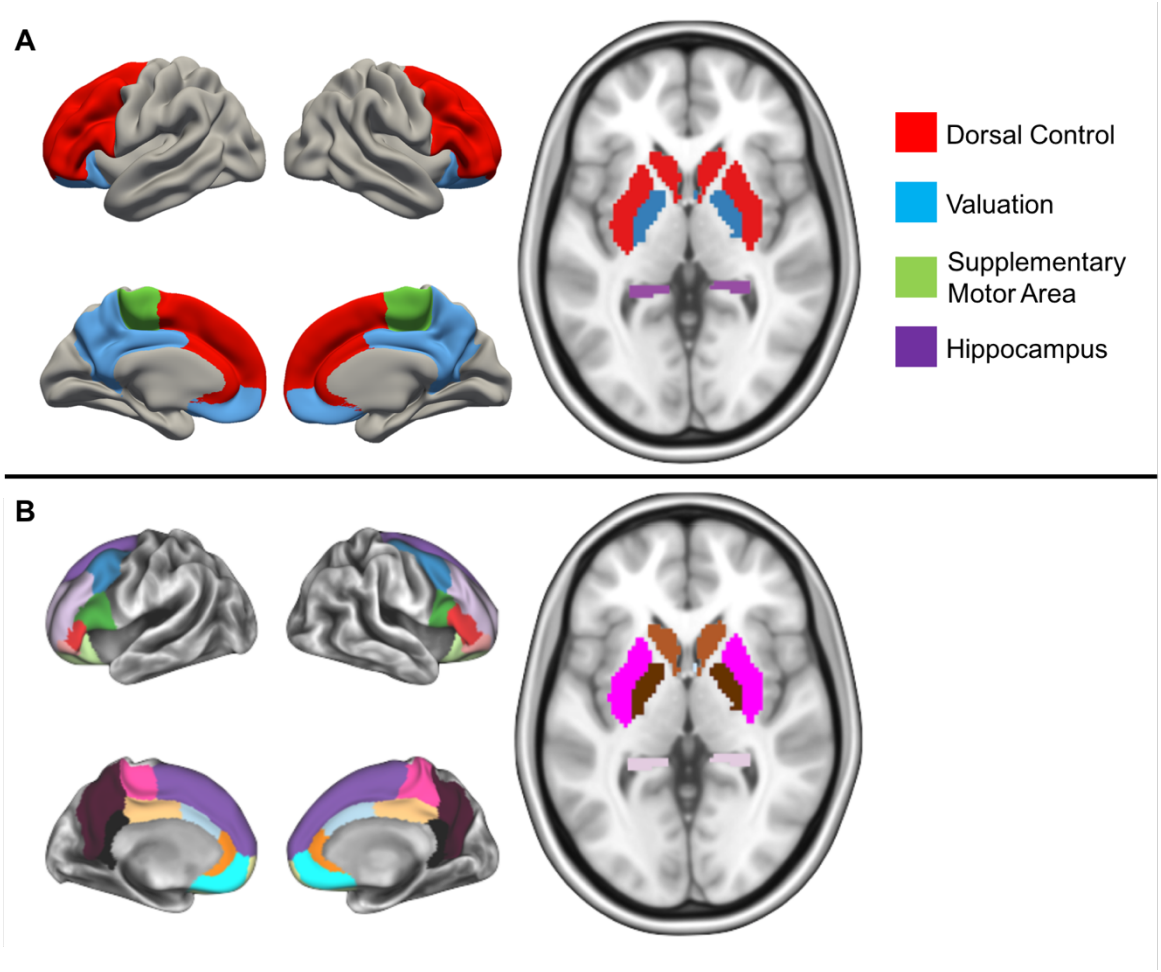

375

376 **Figure 1: Brain systems of interest and regions of interest.** [A] Brain networks (including two other
377 regions out of the networks) included in this study. The regions in red represent the cognitive control
378 network. The regions in blue represent the valuation network. The regions in green and purple represent
379 the supplementary motor area and the hippocampus, respectively. [B] Each brain region included in this
380 study.

381

382 *Statistical analysis*

383 In this study, we first tested to see whether chronological age could be used to predict temporal
384 discounting preference as measured by AUC. We then tested to see if the strength of connectivity
385 between each of our ROIs was able to explain variance in temporal discounting AUC values

386 above chronological age. All analyses were conducted in R version >3.3.3 (https://www.r-
387 project.org/). The script we used to conduct these analyses is freely available online to facilitate
388 reproducibility and replication efforts (https://github.com/katemills/temporal_discounting).
389
390 *Sample 1*
391 For our first, longitudinal, sample we tested each of these questions using mixed-effects models
392 with the nlme package implemented through R. Mixed effects modeling accounts for the non-
393 independence of the data collected from the same individual over time, and allows for unequal
394 spacing between data collection points. This statistical analysis contains both the average slope
395 and intercepts of the parameter (fixed effects), and varying intercept for each individual that is a
396 random deviation of the fixed effect (random effect). We tested the following three polynomial
397 models to predict AUC from chronological age:

398 Linear age model: $y = \beta_0 + \beta_1(x)$

399 Quadratic age model: $y = \beta_0 + \beta_1(x) + \beta_2(x^2)$

400 Cubic age model: $y = \beta_0 + \beta_1(x) + \beta_2(x^2) + \beta_3(x^3)$

401 Where y is the AUC value, and β_0 represents the intercept; x represents the participant's age;
402 and $\beta_1, \beta_2 \, and \, \beta_3$ represent regression coefficients. We centered age for all analyses (10.70
403 years). The three age models were compared and tested against a null model that only included
404 the random intercept for each individual. The best fitting model was determined by Akaike
405 Information Criterion (AIC) and likelihood ratio (LR) statistics using the heuristic of parsimony.
406 The model with the lowest AIC value that was significantly different (p<.05), as determined
407 from LR tests, from less complex models was chosen.
408

409 To identify the connections that could predict an individual's AUC score above chronological
410 age, we used LR statistics to compare models including a connection of interest (COI)
411 correlation coefficient as an interaction and/or main effect added to the age only model. These
412 brain connectivity models were then compared against each other as well as the best fitting age
413 model. The model with the lowest AIC value that was significantly different (p<.01) from less
414 complex models was selected as the best fitting model. To account for the possibility that brain
415 connectivity alone could account for more variance in AUC values than the age-only model or
416 the multivariate models, we also tested to see if a model including the COI correlation
417 coefficient, but not age, was the best fitting model. We identified connectivity-only models if
418 they had lower AIC than the age only models, and were also both significantly different and had
419 lower AIC than the other more complex models.
420
421 *Sample 2*
422 We examined the same questions in the second sample to test the replicability of the results
423 obtained from the first sample. Similar to our first sample, we first examined the relationship
424 between AUC and chronological age, specifically by comparing linear to nonlinear models
425 (quadratic & cubic). Since these data were cross-sectional, we used regular linear regression to
426 fit these models and compared models through F tests (p<.05). Age was centered for all analyses
427 (10.23 years). Once the best age model was determined, we tested if adding COI correlation
428 coefficients to the model would improve the model fit through F tests (p<.05). We only
429 examined the COIs that were determined to explain additional variance in AUC above age in the
430 first sample.
431

Results

AUC increases from late childhood into early adolescence

Model comparisons between the null, linear age, quadratic age, and cubic age models are presented in **Table 2**. Of the three age models tested, the quadratic model best represented the relationship between age and AUC in this longitudinal sample (LR quadratic model vs. null: 13.2, $p < .002$). The results of this model suggest that, on average, each yearly increase in age across this sample was associated with an increase of 0.04 AUC, with a negative rate of change (-0.01) (**Table 3; Figure 2**). These results should be interpreted from the predicted intercept at age 10.70 years (0.55). The graph illustrates a group-level increase in AUC until age ~11 years, but relative stability in AUC between ages 11-14 years.

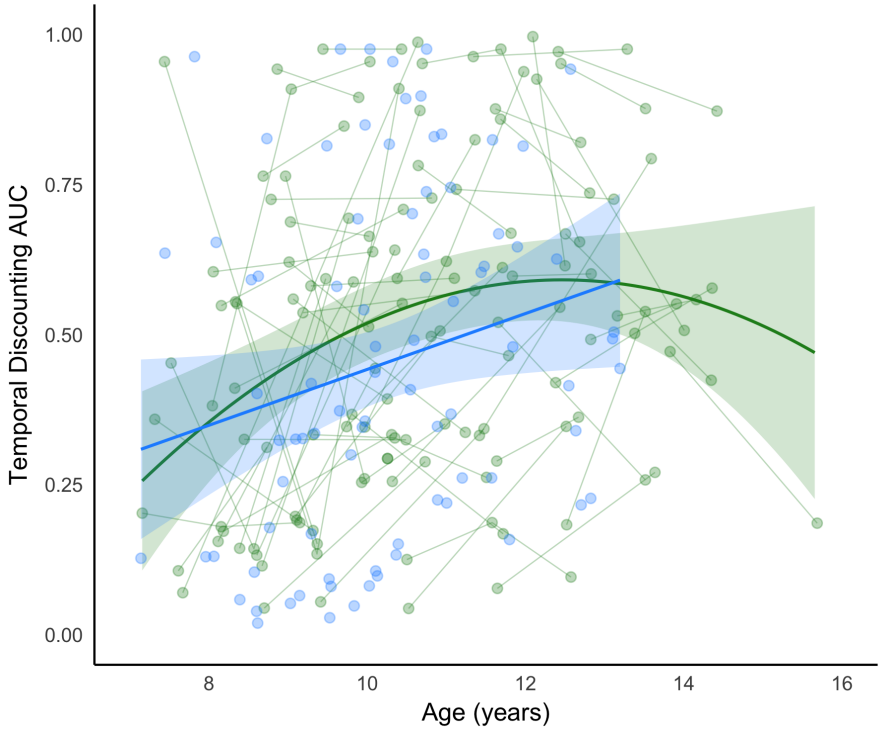

Figure 2: Best fitting age models for AUC. The green line represents the predicted model fit for AUC for sample 1 (longitudinal sample) and the blue line represents the predicted model fit for AUC for

sample 2 (cross-sectional sample). Shading represents the 95% confidence intervals. Raw data are plotted in the background, with each individual measurement representing a circle, and lines connecting data collected from the same individual across time.

In our second, cross-sectional, sample, we found evidence for a linear relationship between age and AUC (**Figure 2**; blue). The linear model for this sample suggests that, on average, each yearly increase in age across this sample was associated with an increase of 0.05 AUC (**Table 3; Figure 2**). These results should be interpreted from the predicted intercept at age 10.23 years (0.45). Overall, the graph shows a similar increase in AUC across the age period studied as is visible in the longitudinal sample.

Table 2. Comparison of polynomial age models for the longitudinal sample.

Longitudinal sample								
	Model	df	AIC	BIC	logLik	Test	L.Ratio	p-value
Null Model	1	3	25.0	33.7	-9.5			
Linear Age	2	4	18.8	30.4	-5.4	1 vs 2	8.2	0.0042
Quadratic Age	3	5	15.8	30.4	-2.9	2 vs 3	5.0	0.0257
Cubic Age	4	6	15.4	32.9	-1.7	3 vs 4	2.4	0.1226

Table 3. Fixed effects for best fitting (quadratic) age model predicting AUC for the longitudinal sample.

Longitudinal Sample					
	Value	Std. Error	DF	t-value	p-value
Intercept	0.55	0.03	71	17.0	<0.0001
Linear age	0.04	0.01	71	3.2	0.0021
Quadratic age	-0.01	0.01	71	-2.2	0.0291

Brain connectivity explains variance in AUC not accounted for by age

In the first sample, we found that AUC was best predicted by models including both age and connectivity for fifty-eight COIs **(SI Table 2)**. Many of the connections (40%) were between regions within the cognitive control network, whereas 10% of connections were between regions within the valuation network. 36% of the connections were between the cognitive control network regions and the valuation network regions. None of the identified connections included connections between the control network and the SMA or the hippocampus, however, one connection between the valuation network and hippocampus and three connections between the valuation and the SMA were identified as relevant to predicting AUC. All four possible connections between the SMA and hippocampus were identified as relevant to predicting AUC.

Of the fifty-eight connections identified in the first sample, only nine were replicated in the cross-sectional sample (**Table 4; Figure 3**). Three of the nine connections represented connections within regions of the cognitive control system (left dlPFC – right dACC; bilateral dlPFC; bilateral superior frontal cortex); three represented connections within regions of the valuation system (right pallidum – left PCC; right pallidum – right PCC; right mOFC – left amygdala); and three represented connections between these two systems (left dlPFC – right PCC; left superior frontal cortex – right PCC; left mOFC – right vlPFC). Model statistics for these nine models are detailed for both the longitudinal sample and cross-sectional sample in **Table 4**.

The majority of the identified connections showed similar effects across samples. The three connections within the cognitive control system impacted the prediction of AUC similarly in both samples: individuals with greater connectivity strength between these cognitive control

regions were predicted to have a preference for LLR (higher AUC) across the age ranges studied. The beta values for the main effect of connectivity were similar across the samples as well, with connectivity beta estimates ranging from 0.26 – 0.37 for the longitudinal sample, and 0.30 – 0.42 for the cross-sectional sample.

The three connections within the valuation system also impacted the prediction of AUC similarly in both samples: individuals with greater connectivity strength between these valuation regions were predicted to have a preference for the SSR (lower AUC) across the age ranges studied. The beta values for the main effect of connectivity were similar across the samples as well, with connectivity beta estimates ranging from -0.38 – -0.23 for the longitudinal sample, and -0.58 – -0.27 for the cross-sectional sample. The impact of connectivity between the right pallidum and PCC on predicting AUC with age was virtually identical for both cortical hemispheres.

Individuals with greater connectivity strength between the left mOFC and right vlPFC were predicted to have a preference for LLR (higher AUC) across the age ranges studied, similar to patterns found for connections between the cognitive control regions. Connectivity between these two regions was a better predictor of AUC than age alone in the cross-sectional sample. Within the longitudinal sample, connectivity strength between the right PCC and the left dlPFC or left superior frontal cortex interacted with the quadratic age term to predict AUC, with stronger connectivity strength predicting a preference for LLR (higher AUC) only at the tail ends of the age range. Within the cross-sectional sample, participants greater connectivity strength between the right PCC and left dlPFC were predicted to have a preference for LLR (higher AUC). Connectivity between the right PCC and left superior frontal cortex was a better predictor

509 of AUC than age alone in the cross-sectional sample, with individual with greater connectivity

510 strength between these regions having a preference for LLR (higher AUC).

Table 4. Best fitting model characteristics for the nine connections of interest that replicated across the both samples.

		Longitudinal sample							
Connection	**Networks**	**Best Fit Model**	**LR test**	**AIC diff.**	**Intercept (SE)**	**Linear age Estimate (SE)**	**Quadratic age Estimate (SE)**	**Connectivity Estimate (SE)**	**Quadratic age x Connectivity (SE)**
Left dlPFC – Right dACC	Control – Control	main effect	$X^2(1) = 7.13$, $p = 0.0076$	5.13	0.59 (0.03)	0.05 (0.01)	-0.01 (0.01)	0.26 (0.1)	-
Left dlPFC – Right dlPFC	Control – Control	main effect	$X^2(1) = 8.68$, $p = 0.0032$	6.68	0.4 (0.06)	0.05 (0.01)	-0.01 (0.01)	0.36 (0.12)	-
Left Superior Frontal Cortex – Right Superior Frontal Cortex	Control – Control	main effect	$X^2(1) = 8.95$, $p = 0.0028$	6.95	0.36 (0.07)	0.05 (0.01)	-0.01 (0.01)	0.37 (0.12)	-
Right Pallidum – Right PCC	Valuation – Valuation	main effect	$X^2(1) = 8.27$, $p = 0.004$	6.27	0.56 (0.03)	0.05 (0.01)	-0.01 (0.01)	-0.34 (0.11)	-
Right Pallidum – Left PCC	Valuation – Valuation	main effect	$X^2(1) = 8.74$, $p = 0.0031$	6.74	0.54 (0.03)	0.05 (0.01)	-0.01 (0.01)	-0.38 (0.12)	-
Right mOFC – Left Amygdala	Valuation – Valuation	quadratic interaction	$X^2(2) = 9.97$, $p = 0.0069$	5.97	0.59 (0.04)	0.04 (0.01)	-0.02 (0.01)	-0.23 (0.15)	0.09 (0.03)
Left dlPFC – Right PCC	Control – Valuation	quadratic interaction	$X^2(2) = 11.44$, $p = 0.0033$	7.44	0.54 (0.03)	0.06 (0.01)	-0.01 (0.01)	-0.08 (0.11)	0.1 (0.03)
Left Superior Frontal Cortex – Right PCC	Control – Valuation	quadratic interaction	$X^2(2) = 9.9$, $p = 0.0071$	5.9	0.55 (0.03)	0.06 (0.01)	-0.01 (0.01)	-0.2 (0.12)	0.1 (0.03)
Left mOFC – Right vlPFC	Valuation – Control	main effect	$X^2(1) = 7.13$, $p = 0.0076$	5.13	0.51 (0.04)	0.04 (0.01)	-0.01 (0.01)	0.27 (0.1)	-

		Cross-sectional sample					
Connection	**Networks**	**Best Fit Model**	**F test**	**adj R Sq**	**Intercept (SE)**	**Linear age (SE)**	**Connectivity (SE)**
Left dlPFC – Right dACC	Control – Control	main effect	$F(2,81) = 5.13$, p = 0.0203	0.09	0.51 (0.04)	0.05 (0.02)	0.3 (0.13)
Left dlPFC – Right dlPFC	Control – Control	main effect	$F(2,81) = 4.99$, p = 0.0233	0.09	0.28 (0.08)	0.05 (0.02)	0.42 (0.18)
Left Superior Frontal Cortex – Right Superior Frontal Cortex	Control – Control	main effect	$F(2,81) = 4.92$, p = 0.025	0.09	0.25 (0.1)	0.05 (0.02)	0.40 (0.18)
Right Pallidum – Right PCC	Valuation – Valuation	main effect	$F(2,81) = 6.21$, $p = 0.007$	0.11	0.46 (0.03)	0.04 (0.02)	-0.53 (0.19)
Right Pallidum – Left PCC	Valuation – Valuation	main effect	$F(2,81) = 6.72$, $p = 0.0043$	0.12	0.45 (0.03)	0.05 (0.02)	-0.58 (0.2)
Right mOFC – Left Amygdala	Valuation – Valuation	main effect	F(2,81) = 4.62, $p = 0.0342$	0.08	0.47 (0.03)	0.05 (0.02)	-0.27 (0.12)
Left dlPFC – Right PCC	Control – Valuation	main effect	$F(2,81) = 4.4$, p = 0.043	0.08	0.48 (0.03)	0.05 (0.02)	0.28 (0.14)
Left Superior Frontal Cortex – Right PCC	Control – Valuation	coi only	$F(1,82) = 6.18$, $p = 0.015$	0.06	0.44 (0.03)	-	0.37 (0.15)
Left mOFC – Right vlPFC	Valuation – Control	coi only	F(1,82) = 6.27, $p = 0.0142$	0.06	0.41 (0.03)	-	0.35 (0.14)

Discussion

In this study, we investigated whether individual differences in functional brain organization are associated with temporal discounting preferences in the transition into adolescence. Specifically, we tested if functional connectivity between regions involved in valuation, cognitive control, hippocampus and SMA could explain variance in temporal discounting preference (AUC) above chronological age. To ensure validity of our reported results, we tested these models in two independent datasets: a longitudinal dataset of children aged 7-15 years and a cross-sectional dataset of 7-13 year olds.

In both samples we observed a group-average increase in AUC between late childhood and early adolescence. We found evidence that the relationship between age and AUC was best represented by a quadratic trajectory in our longitudinal sample, with AUC increasing between ages 7-11 years before stabilizing. For the cross-sectional sample, we identified a linear increase in AUC between ages 7-13 years. While the best fitting model differed between these samples, the overall pattern observed in both samples reflected a general trend for our participants to prefer waiting for a later, larger reward (LLR) as they got older.

This result supports the general finding that temporal discounting preferences shift in the transition into adolescence (Achterberg et al., 2016; Scheres et al., 2014). Scheres et al., (2014) demonstrated in a cross-sectional sample encompassing ages 6-19 years that adolescents were more likely to wait for the LLR in comparison to children and young adults. Achterberg et al., (2016) similarly found that the ability to delay gratification increased from childhood into adolescence. It is important to note that, although we found a group-average increase in AUC

534 across the transition into adolescence, there was substantial individual variability (see **Figure 2**).
535 Further, because our sample age range ends at 15 years we cannot be sure if the preference for
536 LLR declines between mid-to-late adolescence.
537
538 *Individual differences in functional connectivity are related to temporal discounting preference*
539 The current study proposed that individual variability in temporal discounting preference could
540 be explained by differences in intrinsic functional organization. To test this hypothesis, we
541 examined if intrinsic functional connectivity between a set of *a priori* regions of interest and
542 networks could improve the "age only" models in predicting an individual's temporal
543 discounting preference. To mitigate false positives and overfitting, we implemented both a
544 stringent model selection procedure utilizing AIC as well as Likelihood Ratio tests paired with
545 replication in an independent sample. We found nine distinct brain connections were able to
546 explain variance in temporal discounting preference above age alone in both our longitudinal and
547 cross-sectional samples. These findings suggest that individual differences in functional brain
548 connectivity can explain a portion of individual variability in temporal discounting preferences
549 during the transition to adolescence.
550
551 Our results demonstrate that individuals with greater connectivity between cortical regions
552 within cognitive control systems are more inclined to choose LLR. Specifically, we found that
553 increased connectivity between the left dlPFC and the right dACC, bilateral dlPFC, and bilateral
554 superior frontal cortex, relate to a preference for LLR for individuals across the transition into
555 adolescence (**Figure 3a-c**).

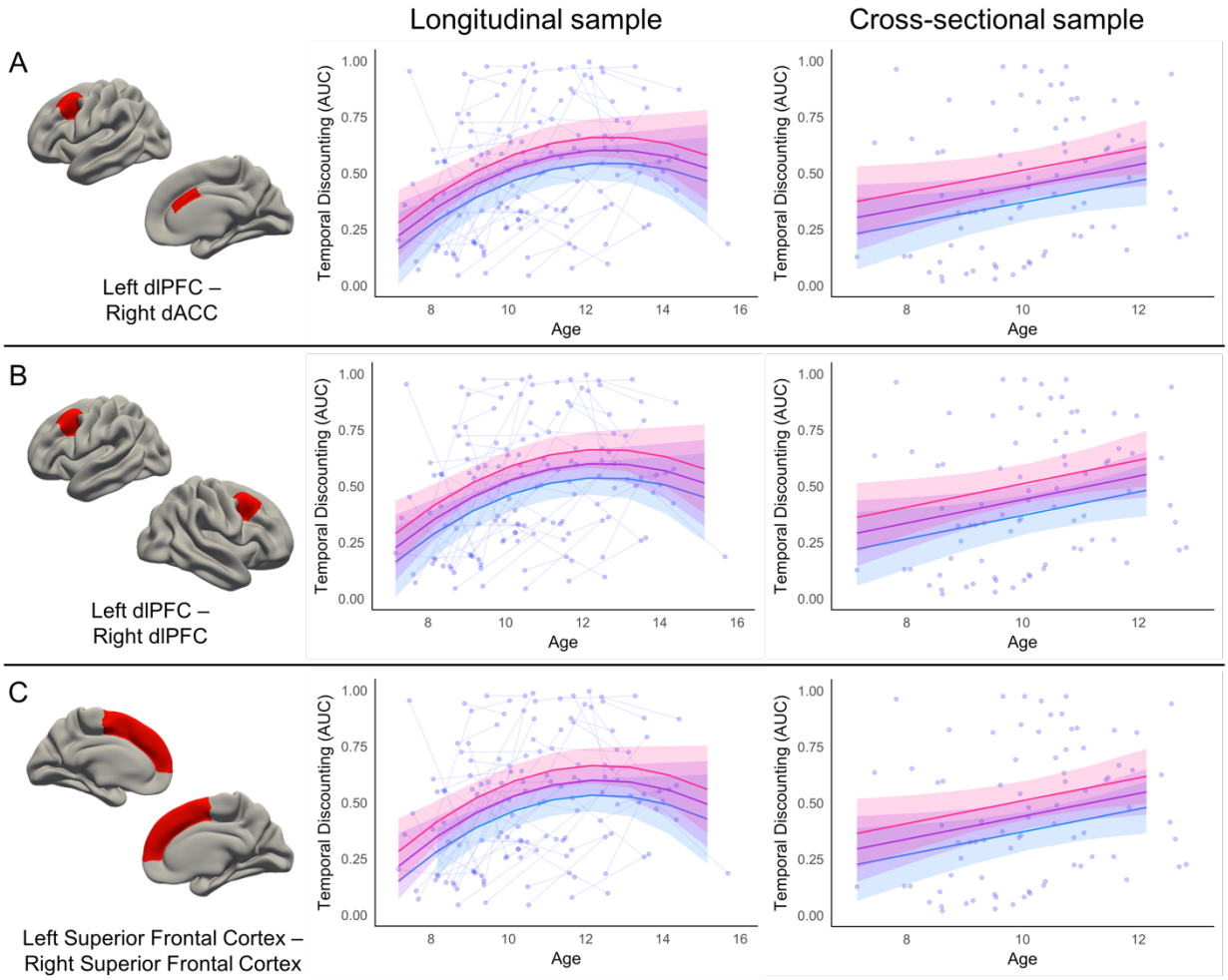

Figure 3a-c: Relationship between cognitive control regions and AUC. The cortical regions involved in the connectivity between two cognitive control systems are represented by red on the brain. Pink trajectory represents AUC for an individual with 1 standard deviation higher connectivity than the mean between the two regions. Purple trajectory represents predicted AUC for participants with the mean connectivity strength between the two regions. Blue trajectory represents AUC for an individual with 1 standard deviation lower connectivity than the mean between the two regions. Raw data are plotted in the background, with each individual measurement representing a circle, and lines connecting data collected from the same individual across time.

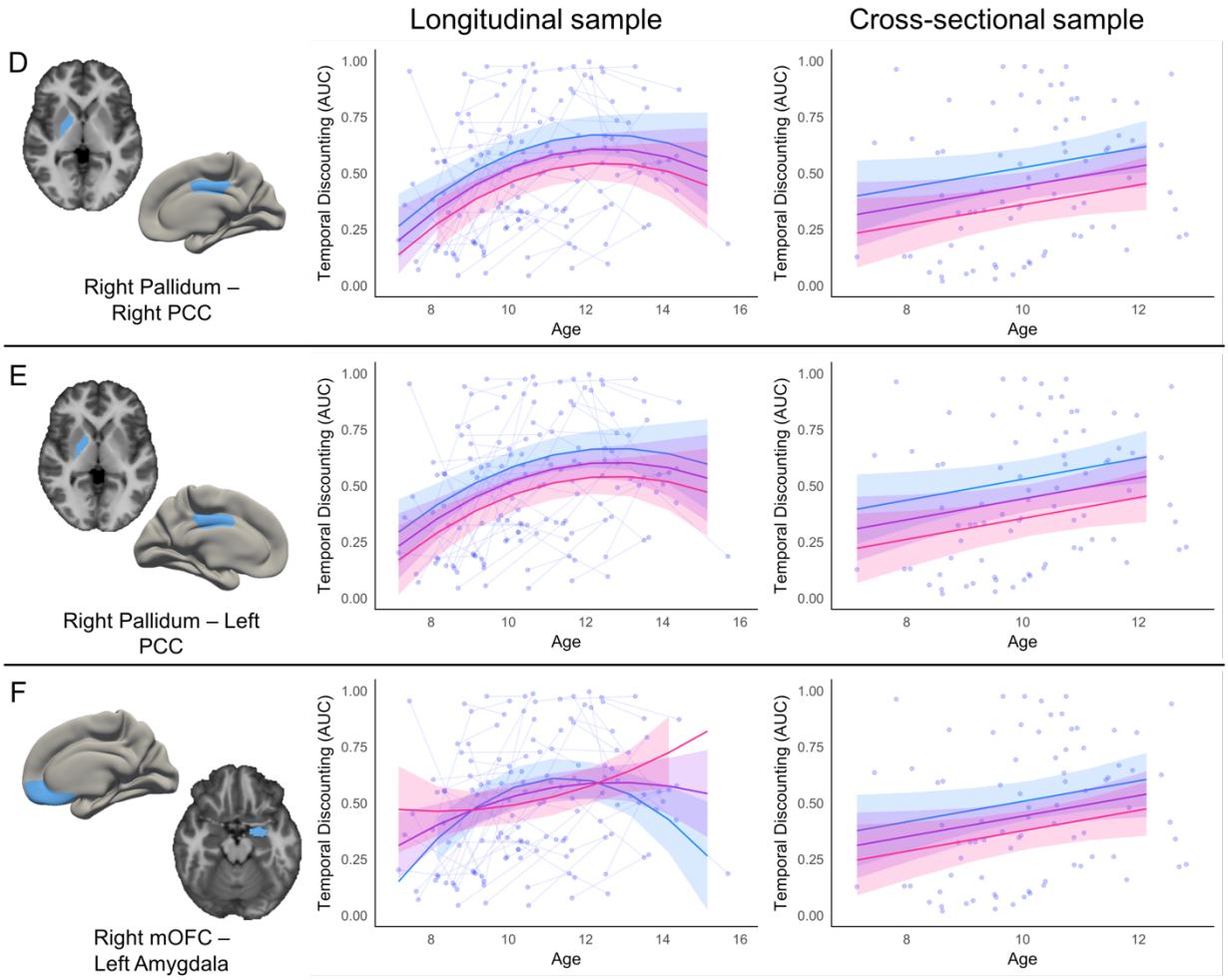

Figure 3d-f: Relationship between valuation regions and AUC. The regions, between cortical and subcortical, involved in the connectivity between two valuation systems are represented by blue on the brain. Pink trajectory represents AUC for an individual with 1 standard deviation higher connectivity than the mean between the two regions. Purple trajectory represents predicted AUC for participants with the mean connectivity strength between the two regions. Blue trajectory represents AUC for an individual with 1 standard deviation lower connectivity than the mean between the two regions. Raw data are plotted in the background, with each individual measurement representing a circle, and lines connecting data collected from the same individual across time.

Across samples, we found evidence that greater connectivity between right pallidum and the bilateral PCC was associated with a preference for SSR across the transition into adolescence. Specifically, a greater connectivity between these valuation regions predicted lower AUC for individuals across the age ranges studied (**Figure 3de**). These results align with previous findings showing individual differences in cortico-striatal circuitry are related to temporal discounting preferences (van den Bos et al., 2014; 2015). Our results also demonstrate that increased connectivity between the left amygdala and right mOFC was related to increased preference for the SSR in the transition to adolescence (**Figure 3f**). While a main effect was found for the cross-sectional sample, there was an interaction between connectivity and the quadratic age term for the longitudinal sample. This presents the possibility that the relationship between increased connectivity between the left amygdala and right mOFC and temporal discounting preference is not static across ages 7-15 years.

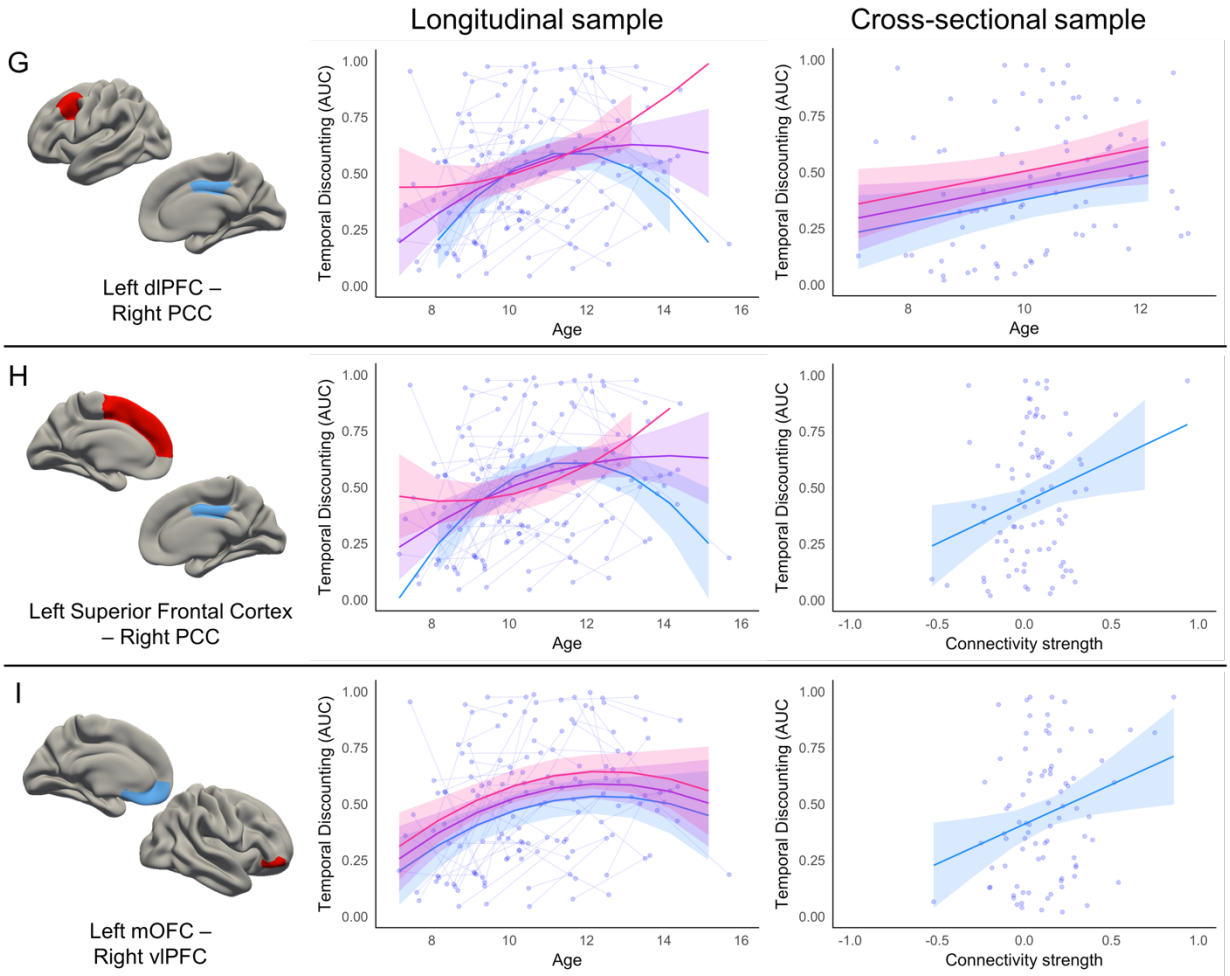

Figure 3g-i: Relationship between valuation network and cognitive control network and AUC. The cortical regions involved in the connectivity between valuation system and cognitive control system are represented by blue and red, respectively, on the brain. The Pink trajectory represents AUC for an individual with 1 standard deviation higher connectivity than the mean between the two regions. Purple trajectory represents predicted AUC for participants with the mean connectivity strength between the two regions. Blue trajectory represents AUC for an individual with 1 standard deviation lower connectivity than the mean between the two regions. Raw data are plotted in the background, with each individual measurement representing a circle, and lines connecting data collected from the same individual across time.

While we found evidence that increased connectivity between the right PCC and the left dlPFC or left superior frontal cortex was related to greater preference for LLR for individuals across ages in the cross-sectional sample, the best fitting models in the longitudinal sample suggested a nonlinear relationship between this strength of these connections and AUC preference across age (**Figure 3gh**). We found that greater connectivity between the left mOFC to right vlPFC (the pars orbitalis region of the inferior frontal gyrus) was related to increased preference for LLR across the transition into adolescence. This possibly reflects that stronger functional connectivity at rest between these regions reflects the ability for the vlPFC/IFG to regulate mOFC signaling (Hare, Camerer, & Rangel, 2009). In both samples, a main effect of greater connectivity between the dlPFC and several regions predicted higher AUC (increased preference for LLR or less discounting) for individuals across the transition into adolescence. This result held for connections between the dlPFC and dACC, bilateral dlPFC, as well as dlPFC and PCC, further underscoring the role of dlPFC in the development of temporal discounting behavior (Wang et al., 2017).

Role of dopaminergic signaling in temporal discounting behavior

All of the identified relevant connections between regions of the valuation network (amygdala, mOFC, PCC, and pallidum) showed a negative relationship with AUC, with stronger connectivity predicting a greater preference for SSR across participants. This could be related to the abundance of dopaminergic signaling in the valuation network. Multiple studies have shown that areas of the brain with dopaminergic innervation are involved in temporal discounting preference (Kobayashi & Schultz, 2008; Pine, Shiner, Seymour, & Dolan, 2010). Furthermore, it has been reported that individuals with increased dopamine release are more inclined to choose

625 the SSR (Joutsa et al., 2015). Crossover work in animal models might allow for direct testing of
626 this hypothesis (Grayson & Fair, 2017; Grayson, Kroenke, Neuringer, & Fair, 2014; Miranda-
627 Dominguez et al., 2014; Stafford et al., 2014).
628
629 One hypothesis is that changes in the cortico-striatal circuitry that occur in the transition into
630 adolescence are related to hormonal changes that affect the interaction within the networks
631 (Blakemore, Burnett, & Dahl, 2010; Chambers, Taylor, & Potenza, 2003). Specifically, these
632 hormonal changes impact and influence motivation towards reward seeking behaviors (Luciana
633 & Collins, 2012). Pubertal hormones and neurotransmitters, such as sex hormones and
634 dopamine, affect regions across the brain, but their effects (especially dopamine) on the vmPFC,
635 NAcc, and caudate might influence the development of cognitive capacities such as abstract
636 thinking, problem solving, and working memory (Chambers et al., 2003).
637
638 *Limitations and Future directions*
639 This study examined temporal discounting preference as it relates to biological measures.
640 However, social environmental factors can impact an individual's subjective value of money and
641 preference for waiting for a LLR. For example, a previous study found that individuals who grew
642 up in lower socio-economic status environments (SES) preferred SSR, whereas individuals who
643 grew up in higher SES environments preferred LLR (Griskevicius et al., 2013). In an
644 experimental manipulation, Kidd, Palmeri, & Aslin (2013) demonstrated that children presented
645 with a reliable environment demonstrated a significant increase in their delay time compared to
646 children presented with an unstable environment. It should not be assumed that steeper
647 discounting is always maladaptive. Very low socio-economic status populations were under-

represented in the current study. Future investigations should assess how social environmental factors might impact the relationship between biological measures and temporal discounting preference.

Previous studies have shown evidence for heterogeneity in functional connectivity existing across individuals in typically developing as well as in clinical samples (Costa Dias et al., 2015; Fair, Bathula, Nikolas, & Nigg, 2012; Gates, Molenaar, Iyer, Nigg, & Fair, 2014). For example, graph theory and community detection can be used to classify typically developing children into specific neuropsychological subgroups (Gates et al., 2014), and functional subgroups can be differentiated based on heterogeneity related to behavioral characteristics including impulsivity (Costa Dias et al., 2015). This study did not account for these heterogeneity present in the group and further investigation should be considerate of this phenomenon. Further, the current study utilized a brain parcellation based on anatomical boundaries (the Desikan-Killiany atlas; Desikan et al., 2006) in order to test hypotheses generated from previous work. However, establishing the consistency of these findings with other parcellations (Glasser et al., 2016; Gordon et al., 2016) will be an important next step (Grayson & Fair, 2017; Hagmann, Grant, & Fair, 2012).

Conclusion

On average, children start to prefer waiting for later, larger rewards as they transition into adolescence. However, there is a substantial amount of variability in temporal discounting preference between individuals across development. This study provides evidence that individual differences in functional brain connectivity within and between regions in cognitive control and valuation networks can account for variance in temporal discounting preference above age.

671 Specifically, greater connectivity strength between cognitive control regions, as well as between
672 cognitive control and valuation regions, was related to a preference for waiting for a larger
673 reward. In contrast, greater connectivity strength between valuation network regions was related
674 to a preference for taking an immediate, smaller, reward. Future studies should examine the
675 impact of social environmental factors on the relationship between functional brain connectivity
676 and temporal discounting behavior across development.

677

678 **Funding**

679 This research was supported by R01 MH107418 (Mills, PI: Pfeifer), DeStefano Innovation Fund
680 (Fair), R01 MH096773 (Fair), MH099064 (Nigg), MH086654 (MPI: Fair, Nigg), and
681 MH086654 (Nigg).

682

683 **Acknowledgements**

684 We would like to thank the participants and families for their ongoing participation in this study,
685 as well as the many staff involved in administrative tasks and data collection of this project.

686

687

References

Achterberg, M., Peper, J. S., van Duijvenvoorde, A. C. K., Mandl, R. C. W., & Crone, E. A. (2016). Frontostriatal White Matter Integrity Predicts Development of Delay of Gratification: A Longitudinal Study. *The Journal of Neuroscience: The Official Journal of the Society for Neuroscience*, *36*(6), 1954–1961. https://doi.org/10.1523/JNEUROSCI.3459-15.2016

Banich, M. T., De La Vega, A., Andrews-Hanna, J. R., Mackiewicz Seghete, K., Du, Y., & Claus, E. D. (2013). Developmental trends and individual differences in brain systems involved in intertemporal choice during adolescence. *Psychology of Addictive Behaviors: Journal of the Society of Psychologists in Addictive Behaviors*, *27*(2), 416–430. https://doi.org/10.1037/a0031991

Blakemore, S.-J., Burnett, S., & Dahl, R. E. (2010). The role of puberty in the developing adolescent brain. *Human Brain Mapping*, *31*(6), 926–933. https://doi.org/10.1002/hbm.21052

Boly, M., Phillips, C., Tshibanda, L., Vanhaudenhuyse, A., Schabus, M., Dang-Vu, T. T., … Laureys, S. (2008). Intrinsic brain activity in altered states of consciousness: how conscious is the default mode of brain function? *Annals of the New York Academy of Sciences*, *1129*, 119–129. https://doi.org/10.1196/annals.1417.015

Burgess, G. C., Kandala, S., Nolan, D., Laumann, T. O., Power, J. D., Adeyemo, B., … Barch, D. M. (2016). Evaluation of Denoising Strategies to Address Motion-Correlated Artifacts in Resting-State Functional Magnetic Resonance Imaging Data from the Human Connectome Project. *Brain Connectivity*, *6*(9), 669–680. https://doi.org/10.1089/brain.2016.0435

Calluso, C., Tosoni, A., Pezzulo, G., Spadone, S., & Committeri, G. (2015). Interindividual Variability in Functional Connectivity as Long-Term Correlate of Temporal Discounting. *PLOS ONE*, *10*(3), e0119710. https://doi.org/10.1371/journal.pone.0119710

Casey, B. J. (2015). Beyond simple models of self-control to circuit-based accounts of adolescent behavior. *Annual Review of Psychology*, *66*, 295–319. https://doi.org/10.1146/annurev-psych-010814-015156

Chambers, R. A., Taylor, J. R., & Potenza, M. N. (2003). Developmental neurocircuitry of motivation in adolescence: a critical period of addiction vulnerability. *The American Journal of Psychiatry*, *160*(6), 1041–1052.

Christakou, A., Brammer, M., & Rubia, K. (2011). Maturation of limbic corticostriatal activation and connectivity associated with developmental changes in temporal discounting. *NeuroImage*, *54*(2), 1344–1354. https://doi.org/10.1016/j.neuroimage.2010.08.067

Conners, C. K. (2003). *Conners' rating scales: Revised technical manual.* New York, NY:

721 Multi-Health Systems. Retrieved from https://www.mhs.com/MHS-
722 Assessment?prodname=conners3

723 Costa Dias, T. G., Iyer, S. P., Carpenter, S. D., Cary, R. P., Wilson, V. B., Mitchell, S. H., …
724 Fair, D. A. (2015). Characterizing heterogeneity in children with and without ADHD based on
725 reward system connectivity. *Developmental Cognitive Neuroscience*, *11*, 155–174.
726 https://doi.org/10.1016/j.dcn.2014.12.005

727 Costa Dias, T. G., Wilson, V. B., Bathula, D. R., Iyer, S. P., Mills, K. L., Thurlow, B. L., … Fair,
728 D. A. (2012). Reward circuit connectivity relates to delay discounting in children with attention-
729 deficit/hyperactivity disorder. *European Neuropsychopharmacology: The Journal of the*
730 *European College of Neuropsychopharmacology*.
731 https://doi.org/10.1016/j.euroneuro.2012.10.015

732 Cross, C. P., Copping, L. T., & Campbell, A. (2011). Sex differences in impulsivity: a meta-
733 analysis. *Psychological Bulletin*, *137*(1), 97–130. https://doi.org/10.1037/a0021591

734 Dale, A. M., Fischl, B., & Sereno, M. I. (1999). Cortical Surface-Based Analysis: I.
735 Segmentation and Surface Reconstruction. *NeuroImage*, *9*(2), 179–194.
736 https://doi.org/10.1006/nimg.1998.0395

737 de Water, E., Cillessen, A. H. N., & Scheres, A. (2014). Distinct age-related differences in
738 temporal discounting and risk taking in adolescents and young adults. *Child Development*, *85*(5),
739 1881–1897. https://doi.org/10.1111/cdev.12245

740 Desikan, R. S., Ségonne, F., Fischl, B., Quinn, B. T., Dickerson, B. C., Blacker, D., … Killiany,
741 R. J. (2006). An automated labeling system for subdividing the human cerebral cortex on MRI
742 scans into gyral based regions of interest. *NeuroImage*, *31*(3), 968–980.
743 https://doi.org/10.1016/j.neuroimage.2006.01.021

744 Dosenbach, N. U. F., Koller, J. M., Earl, E. A., Miranda-Dominguez, O., Klein, R. L., Van, A.
745 N., … Fair, D. A. (2017). Real-time motion analytics during brain MRI improve data quality and
746 reduce costs. *NeuroImage*, *161*, 80–93. https://doi.org/10.1016/j.neuroimage.2017.08.025

747 Fair, D. A., Bathula, D., Nikolas, M. A., & Nigg, J. T. (2012). Distinct neuropsychological
748 subgroups in typically developing youth inform heterogeneity in children with ADHD.
749 *Proceedings of the National Academy of Sciences of the United States of America*, *109*(17),
750 6769–6774. https://doi.org/10.1073/pnas.1115365109

751 Fair, D. A., Nigg, J. T., Iyer, S., Bathula, D., Mills, K. L., Dosenbach, N. U. F., … Milham, M.
752 P. (2012). Distinct neural signatures detected for ADHD subtypes after controlling for micro-
753 movements in resting state functional connectivity MRI data. *Frontiers in Systems Neuroscience*,
754 *6*, 80. https://doi.org/10.3389/fnsys.2012.00080

Fischl, B., & Dale, A. M. (2000). Measuring the thickness of the human cerebral cortex from magnetic resonance images. *Proceedings of the National Academy of Sciences*, *97*(20), 11050–11055. https://doi.org/10.1073/pnas.200033797

Fischl, B., Salat, D. H., Busa, E., Albert, M., Dieterich, M., Haselgrove, C., … Dale, A. M. (2002). Whole brain segmentation: automated labeling of neuroanatomical structures in the human brain. *Neuron*, *33*(3), 341–355.

Fischl, B., Sereno, M. I., & Dale, A. M. (1999). Cortical surface-based analysis. II: Inflation, flattening, and a surface-based coordinate system. *NeuroImage*, *9*(2), 195–207. https://doi.org/10.1006/nimg.1998.0396

Fischl, B., van der Kouwe, A., Destrieux, C., Halgren, E., Ségonne, F., Salat, D. H., … Dale, A. M. (2004). Automatically parcellating the human cerebral cortex. *Cerebral Cortex (New York, N.Y.: 1991)*, *14*(1), 11–22.

Gates, K. M., Molenaar, P. C. M., Iyer, S. P., Nigg, J. T., & Fair, D. A. (2014). Organizing heterogeneous samples using community detection of GIMME-derived resting state functional networks. *PloS One*, *9*(3), e91322. https://doi.org/10.1371/journal.pone.0091322

Glasser, M. F., Coalson, T. S., Robinson, E. C., Hacker, C. D., Harwell, J., Yacoub, E., … Van Essen, D. C. (2016). A multi-modal parcellation of human cerebral cortex. *Nature*, *536*(7615), 171–178. https://doi.org/10.1038/nature18933

Glasser, M. F., Sotiropoulos, S. N., Wilson, J. A., Coalson, T. S., Fischl, B., Andersson, J. L., … Jenkinson, M. (2013). The minimal preprocessing pipelines for the Human Connectome Project. *NeuroImage*, *80*(Supplement C), 105–124. https://doi.org/10.1016/j.neuroimage.2013.04.127

Gordon, E. M., Laumann, T. O., Adeyemo, B., Huckins, J. F., Kelley, W. M., & Petersen, S. E. (2016). Generation and Evaluation of a Cortical Area Parcellation from Resting-State Correlations. *Cerebral Cortex (New York, N.Y.: 1991)*, *26*(1), 288–303. https://doi.org/10.1093/cercor/bhu239

Grayson, D. S., & Fair, D. A. (2017). Development of large-scale functional networks from birth to adulthood: A guide to the neuroimaging literature. *NeuroImage*, *160*, 15–31. https://doi.org/10.1016/j.neuroimage.2017.01.079

Grayson, D. S., Kroenke, C. D., Neuringer, M., & Fair, D. A. (2014). Dietary omega-3 fatty acids modulate large-scale systems organization in the rhesus macaque brain. *The Journal of Neuroscience: The Official Journal of the Society for Neuroscience*, *34*(6), 2065–2074. https://doi.org/10.1523/JNEUROSCI.3038-13.2014

Green, L., Myerson, J., & Mcfadden, E. (1997). Rate of temporal discounting decreases with

788 amount of reward. *Memory & Cognition*, *25*(5), 715–723. https://doi.org/10.3758/BF03211314

789 Greve, D. N., & Fischl, B. (2009). Accurate and robust brain image alignment using boundary-
790 based registration. *NeuroImage*, *48*(1), 63–72. https://doi.org/10.1016/j.neuroimage.2009.06.060

791 Griskevicius, V., Ackerman, J. M., Cantú, S. M., Delton, A. W., Robertson, T. E., Simpson, J.
792 A., … Tybur, J. M. (2013). When the economy falters, do people spend or save? Responses to
793 resource scarcity depend on childhood environments. *Psychological Science*, *24*(2), 197–205.
794 https://doi.org/10.1177/0956797612451471

795 Haber, S. N., & Knutson, B. (2009). The Reward Circuit: Linking Primate Anatomy and Human
796 Imaging. *Neuropsychopharmacology*, *35*(1), 4–26. https://doi.org/10.1038/npp.2009.129

797 Hagmann, P., Grant, P. E., & Fair, D. A. (2012). MR connectomics: a conceptual framework for
798 studying the developing brain. *Frontiers in Systems Neuroscience*, *6*, 43.
799 https://doi.org/10.3389/fnsys.2012.00043

800 Hamilton, K. R., Mitchell, M. R., Wing, V. C., Balodis, I. M., Bickel, W. K., Fillmore, M., …
801 Moeller, F. G. (2015). Choice impulsivity: Definitions, measurement issues, and clinical
802 implications. *Personality Disorders*, *6*(2), 182–198. https://doi.org/10.1037/per0000099

803 Hare, T. A., Camerer, C. F., & Rangel, A. (2009). Self-Control in Decision-Making Involves
804 Modulation of the vmPFC Valuation System. *Science*, *324*(5927), 646–648.
805 https://doi.org/10.1126/science.1168450

806 Hare, T. A., Hakimi, S., & Rangel, A. (2014). Activity in dlPFC and its effective connectivity to
807 vmPFC are associated with temporal discounting. *Frontiers in Neuroscience*, *8*.
808 https://doi.org/10.3389/fnins.2014.00050

809 Jenkinson, M., Beckmann, C. F., Behrens, T. E. J., Woolrich, M. W., & Smith, S. M. (2012).
810 FSL. *NeuroImage*, *62*(2), 782–790. https://doi.org/10.1016/j.neuroimage.2011.09.015

811 Johnson, M. W., & Bickel, W. K. (2008). An algorithm for identifying nonsystematic delay-
812 discounting data. *Experimental and Clinical Psychopharmacology*, *16*(3), 264–274.
813 https://doi.org/10.1037/1064-1297.16.3.264

814 Joutsa, J., Voon, V., Johansson, J., Niemelä, S., Bergman, J., & Kaasinen, V. (2015).
815 Dopaminergic function and intertemporal choice. *Translational Psychiatry*, *5*, e491.
816 https://doi.org/10.1038/tp.2014.133

817 Karalunas, S. L., Gustafsson, H. C., Dieckmann, N. F., Tipsord, J., Mitchell, S. H., & Nigg, J. T.
818 (2017). Heterogeneity in development of aspects of working memory predicts longitudinal
819 attention deficit hyperactivity disorder symptom change. *Journal of Abnormal Psychology*,

820 *126*(6), 774–792. https://doi.org/10.1037/abn0000292

821 Kidd, C., Palmeri, H., & Aslin, R. N. (2013). Rational snacking: young children's decision-
822 making on the marshmallow task is moderated by beliefs about environmental reliability.
823 *Cognition*, *126*(1), 109–114. https://doi.org/10.1016/j.cognition.2012.08.004

824 Kobayashi, S., & Schultz, W. (2008). Influence of reward delays on responses of dopamine
825 neurons. *The Journal of Neuroscience: The Official Journal of the Society for Neuroscience*,
826 *28*(31), 7837–7846. https://doi.org/10.1523/JNEUROSCI.1600-08.2008

827 Lee, N. C., de Groot, R. H. M., Boschloo, A., Dekker, S., Krabbendam, L., & Jolles, J. (2013).
828 Age and educational track influence adolescent discounting of delayed rewards. *Frontiers in*
829 *Psychology*, *4*. https://doi.org/10.3389/fpsyg.2013.00993

830 Li, N., Ma, N., Liu, Y., He, X.-S., Sun, D.-L., Fu, X.-M., … Zhang, D.-R. (2013). Resting-state
831 functional connectivity predicts impulsivity in economic decision-making. *The Journal of*
832 *Neuroscience: The Official Journal of the Society for Neuroscience*, *33*(11), 4886–4895.
833 https://doi.org/10.1523/JNEUROSCI.1342-12.2013

834 Luciana, M., & Collins, P. F. (2012). Incentive Motivation, Cognitive Control, and the
835 Adolescent Brain: Is It Time for a Paradigm Shift? *Child Development Perspectives*, *6*(4), 392–
836 399. https://doi.org/10.1111/j.1750-8606.2012.00252.x

837 Miranda-Dominguez, O., Mills, B. D., Grayson, D., Woodall, A., Grant, K. A., Kroenke, C. D.,
838 & Fair, D. A. (2014). Bridging the gap between the human and macaque connectome: a
839 quantitative comparison of global interspecies structure-function relationships and network
840 topology. *The Journal of Neuroscience: The Official Journal of the Society for Neuroscience*,
841 *34*(16), 5552–5563. https://doi.org/10.1523/JNEUROSCI.4229-13.2014

842 Mitchell, S. H., Wilson, V. B., & Karalunas, S. L. (2015). Comparing hyperbolic, delay-amount
843 sensitivity and present-bias models of delay discounting. *Behavioural Processes*, *114*, 52–62.
844 https://doi.org/10.1016/j.beproc.2015.03.006

845 Myerson, J., & Green, L. (1995). Discounting of delayed rewards: Models of individual choice.
846 *Journal of the Experimental Analysis of Behavior*, *64*(3), 263–276.
847 https://doi.org/10.1901/jeab.1995.64-263

848 Myerson, J., Green, L., & Warusawitharana, M. (2001). Area under the curve as a measure of
849 discounting. *Journal of the Experimental Analysis of Behavior*, *76*(2), 235–243.
850 https://doi.org/10.1901/jeab.2001.76-235

851 Odum, A. L. (2011). Delay Discounting: I'm a k, You're a k. *Journal of the Experimental*
852 *Analysis of Behavior*, *96*(3), 427–439. https://doi.org/10.1901/jeab.2011.96-423

Olson, E. A., Collins, P. F., Hooper, C. J., Muetzel, R., Lim, K. O., & Luciana, M. (2009). White Matter Integrity Predicts Delay Discounting Behavior in 9- to 23-Year-Olds: A Diffusion Tensor Imaging Study. *Journal of Cognitive Neuroscience*, *21*(7), 1406–1421. https://doi.org/10.1162/jocn.2009.21107

Peters, J., & Büchel, C. (2010). Episodic future thinking reduces reward delay discounting through an enhancement of prefrontal-mediotemporal interactions. *Neuron*, *66*(1), 138–148. https://doi.org/10.1016/j.neuron.2010.03.026

Peters, J., & Büchel, C. (2011). The neural mechanisms of inter-temporal decision-making: understanding variability. *Trends in Cognitive Sciences*, *15*(5), 227–239. https://doi.org/10.1016/j.tics.2011.03.002

Pine, A., Shiner, T., Seymour, B., & Dolan, R. J. (2010). Dopamine, Time, and Impulsivity in Humans. *Journal of Neuroscience*, *30*(26), 8888–8896. https://doi.org/10.1523/JNEUROSCI.6028-09.2010

Power, J. D., Barnes, K. A., Snyder, A. Z., Schlaggar, B. L., & Petersen, S. E. (2012). Spurious but systematic correlations in functional connectivity MRI networks arise from subject motion. *NeuroImage*, *59*(3), 2142–2154. https://doi.org/10.1016/j.neuroimage.2011.10.018

Power, J. D., Mitra, A., Laumann, T. O., Snyder, A. Z., Schlaggar, B. L., & Petersen, S. E. (2014). Methods to detect, characterize, and remove motion artifact in resting state fMRI. *NeuroImage*, *84*, 320–341. https://doi.org/10.1016/j.neuroimage.2013.08.048

Power, J. D., Schlaggar, B. L., & Petersen, S. E. (2014). Studying Brain Organization via Spontaneous fMRI Signal. *Neuron*, *84*(4), 681–696. https://doi.org/10.1016/j.neuron.2014.09.007

Puig-Antich, J., & Ryan, N. (1986). *Schedule for Affective Disorders and Schizophrenia for School-Age Children*. Pittsburgh, PA: Western Psychiatric Institute and Clinic.

Richards, J. B., Zhang, L., Mitchell, S. H., & de Wit, H. (1999). Delay or probability discounting in a model of impulsive behavior: effect of alcohol. *Journal of the Experimental Analysis of Behavior*, *71*(2), 121–143. https://doi.org/10.1901/jeab.1999.71-121

Sadaghiani, S., & Kleinschmidt, A. (2013). Functional interactions between intrinsic brain activity and behavior. *NeuroImage*, *80*, 379–386. https://doi.org/10.1016/j.neuroimage.2013.04.100

Scheres, A., de Water, E., & Mies, G. W. (2013). The neural correlates of temporal reward discounting. *Wiley Interdisciplinary Reviews. Cognitive Science*, *4*(5), 523–545. https://doi.org/10.1002/wcs.1246

886 Scheres, A., Tontsch, C., Thoeny, A. L., & Sumiya, M. (2014). Temporal reward discounting in
887 children, adolescents, and emerging adults during an experiential task. *Developmental*
888 *Psychology*, *5*, 711. https://doi.org/10.3389/fpsyg.2014.00711

889 Smith, S. M., Jenkinson, M., Woolrich, M. W., Beckmann, C. F., Behrens, T. E. J., Johansen-
890 Berg, H., … Matthews, P. M. (2004). Advances in functional and structural MR image analysis
891 and implementation as FSL. *NeuroImage*, *23 Suppl 1*, S208-219.
892 https://doi.org/10.1016/j.neuroimage.2004.07.051

893 Stafford, J. M., Jarrett, B. R., Miranda-Dominguez, O., Mills, B. D., Cain, N., Mihalas, S., …
894 Fair, D. A. (2014). Large-scale topology and the default mode network in the mouse
895 connectome. *Proceedings of the National Academy of Sciences of the United States of America*,
896 *111*(52), 18745–18750. https://doi.org/10.1073/pnas.1404346111

897 Steinberg, L., Graham, S., O'Brien, L., Woolard, J., Cauffman, E., & Banich, M. (2009). Age
898 differences in future orientation and delay discounting. *Child Development*, *80*(1), 28–44.
899 https://doi.org/10.1111/j.1467-8624.2008.01244.x

900 van den Bos, W., & McClure, S. M. (2013). Towards a general model of temporal discounting.
901 *Journal of the Experimental Analysis of Behavior*, *99*(1), 58–73. https://doi.org/10.1002/jeab.6

902 van den Bos, W., Rodriguez, C. A., Schweitzer, J. B., & McClure, S. M. (2014). Connectivity
903 Strength of Dissociable Striatal Tracts Predict Individual Differences in Temporal Discounting.
904 *The Journal of Neuroscience*, *34*(31), 10298–10310. https://doi.org/10.1523/JNEUROSCI.4105-
905 13.2014

906 van den Bos, W., Rodriguez, C. A., Schweitzer, J. B., & McClure, S. M. (2015). Adolescent
907 impatience decreases with increased frontostriatal connectivity. *Proceedings of the National*
908 *Academy of Sciences*, *112*(29), E3765–E3774. https://doi.org/10.1073/pnas.1423095112

909 Volkow, N. D., & Baler, R. D. (2015). NOW vs LATER brain circuits: implications for obesity
910 and addiction. *Trends in Neurosciences*, *38*(6), 345–352.
911 https://doi.org/10.1016/j.tins.2015.04.002

912 Wang, S., Zhou, M., Chen, T., Yang, X., Chen, G., & Gong, Q. (2017). Delay discounting is
913 associated with the fractional amplitude of low-frequency fluctuations and resting-state
914 functional connectivity in late adolescence. *Scientific Reports*, *7*(1), 10276.
915 https://doi.org/10.1038/s41598-017-11109-z

916 Wechsler, D. (2003). *Wechsler Intelligence Scale for Children, 4th ed., (WISC-IV) technical and*
917 *interpretive manual.* San Antonio, TX: Harcourt Brace.

918 Woolrich, M. W., Jbabdi, S., Patenaude, B., Chappell, M., Makni, S., Behrens, T., … Smith, S.

M. (2009). Bayesian analysis of neuroimaging data in FSL. *NeuroImage*, *45*(1 Suppl), S173-186. https://doi.org/10.1016/j.neuroimage.2008.10.055

Yi, R., Pitcock, J. A., Landes, R. D., & Bickel, W. K. (2010). The short of it: abbreviating the temporal discounting procedure. *Experimental and Clinical Psychopharmacology*, *18*(4), 366–374. https://doi.org/10.1037/a0019904